Journal of Sound and Vibration (1998) **218**(3), 445–461
Article No. sv981828

INTELLIGENT BEAM TRANSFORMING EARTHQUAKE FORCE INTO VIBRATION CONTROL FORCE AND ITS OPTIMAL DESIGN

K. Nagaya and T. Fukushima

Department of Mechanical Engineering, *Gunma University*, *Kiryu*, *Gunma* 376, *Japan*

(*Received* 23 *February* 1998, *and in final form* 16 *June* 1998)

This paper presents a method of vibration control for a beam carrying a mass at its tip subjected to earthquakes. A vibration isolation mechanism consisting of a gear train for the beam is presented. Theoretical analysis for the beam is developed, and to validate the method and analysis, experimental tests are carried out for a model of the present mechanism. It is clarified that the vibration displacements and the moments in the beam are suppressed significantly in comparison with a general beam without the mechanism. A method of optimal design has also been presented, and numerical calculations have been carried out for the beam with actual sizes. In the present beam, energies for controlling vibrations are not required, because the earthquake force is utilized as a control force. Therefore, the structure using the beam has advantages as compared with the structure having an active vibration control system.

1. INTRODUCTION

In the Hanshin-Awaji earthquake in Japan, a number of structures and buildings were destroyed. To suppress vibrations of structures and buildings, various methods have been reported. Xue *et al*. [1] presented an intelligent passive vibration control system, in which an ordinary passive system is combined to an additional intelligent passive part. Prendergast [2] reported a base isolation system, and discussed vibration isolation of bridges. A numerical simulation was also carried out to assess the effectiveness of a passive isolator, an active vibration absorber, and an integrated passive/active control in the paper given by Lee-Glauser *et al*. [3]. Villaverde Koyama and Leslie [4] discussed a tuned mass–spring–dashpot system. In the paper, the displacement of the roof is reduced by up to about 40% for a 10-story building. A method of tuned mass dampers for seismic applications was also discussed by Sadek *et al*. [5]. Utku *et al*. [6]

0022–460X/98/480445 + 17 $30.00/0

presented a method in which gravitational energy of the mass of the building was used to achieve active vibration control. Active control of flexural structures was discussed by Ohsumi and Sawada [7]. They discussed a method of optimal control system. Chuang *et al*. investigated the LQR control method [8], and Feng and Mita [9] discussed an innovative vibration control system for reducing the dynamic response of tall buildings due to wind and seismic load. The other method is to strengthen the structures. The method is simple because the strength of structures increases with their thickness, but the cost increases with the thickness as well. Columns and beams without walls used in highway bridges and perking were destroyed by the earthquakes. If one of the important elements of a structure is destroyed, the structure is also destroyed, so it is important to prevent destruction of elements such as beams and columns.

Earthquakes have significantly large energies, so if their energies are applicable in the control of structures, vibrations due to earthquakes can be suppressed without increasing the thickness of the structures. But few studies espousing this standpoint have been reported. Hence, the present article discusses a method for reducing the displacements and the bending moments in the beam by using an earthquake force as a control force. To transform the earthquake force into the control force, a gear train mechanism is inserted in a hollow pipe. In the mechanism, an inertia force of the mass at the tip of the beam is transformed into a control moment. Theoretical analyses have been made for the proposed vibration control system. To validate the present method and analyses, experimental tests have been performed.

2. PRINCIPLE OF THE INTELLIGENT BEAM USING THE EARTHQUAKE FORCES AS CONTROL FORCES

Figure 1 depicts the proposed beam in which the earthquake force is transformed into vibration control force. The beam consists of a hollow pipe and a gear train. In Figure 1, a rigid arm 0 is rigidly connected to the tip of the beam, and its other end is rigidly connected to a gear 1 by a shaft. The shaft of the middle gear is connected to the beam, but it can rotate freely around its axis. Gear 3 is rigidly connected to the beam. Hence, when the upper end of the beam moves in the right direction, gear 1 connected to the rigid arm moves, and gear 2 rotates corresponding to the movement of gear 1. The rotation of gear 2 is transmitted to gear 3, but since gear 3 is rigidly connected to the beam, the restoring moment M_3 is generated whose direction is opposite to that of the beam displacement. In this system, the restoring moment due to the reaction force Q can be greater than that due to the applied force $2Q$ when the axes of gears are chosen in appropriate positions, and the restoring moment M_3 can be increased by using the gear ratios of the gear train. Since gear 1 does not rotate in this system, a rack gear is also applicable instead of the spur gear of course.

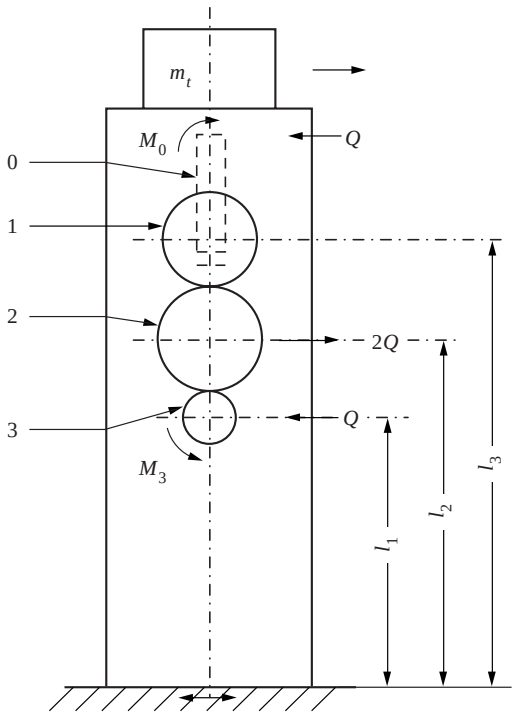

Figure 1. Geometry of the present beam.

3. ANALYSIS

3.1. TRANSFER MATRIX

Figure 2 shows the model of the beam. The beam is divided into a number of elements without mass, and concentrated masses. The transfer matrix method is applied for obtaining vibration response, but in which the effects of axial force on the bending displacement is neglected under the assumption of the bending displacement due to the axial force being small. Then the analysis developed here is also applicable to a column, but the gravity force acting on the column should be small in comparison with its buckling force. Since thick columns are used in standard buildings, shear deformation is considered, and friction forces due to friction between gear teeth are also considered as damping forces.

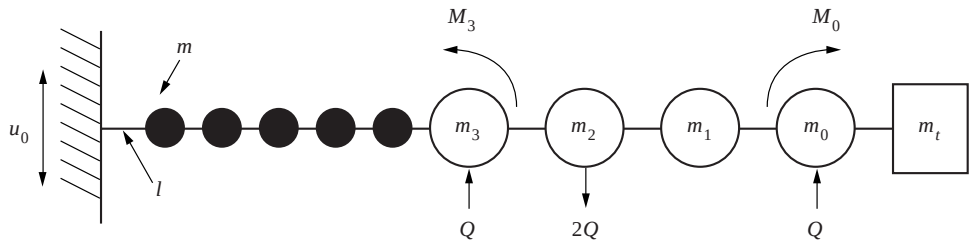

Figure 2. Analytical model.

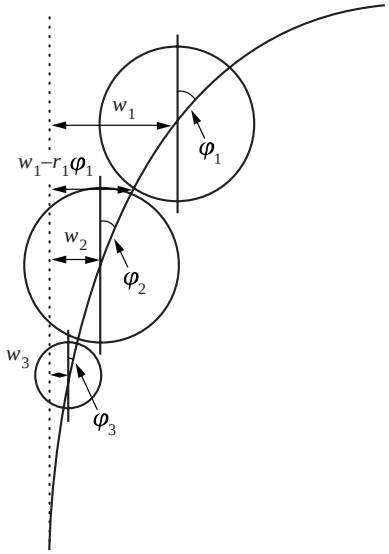

Figure 3. Relation between displacements of the beam and angles of rotation of gears: r_1, radius of gear 1; r_2, radius of gear 2; r_3, radius of gear 3.

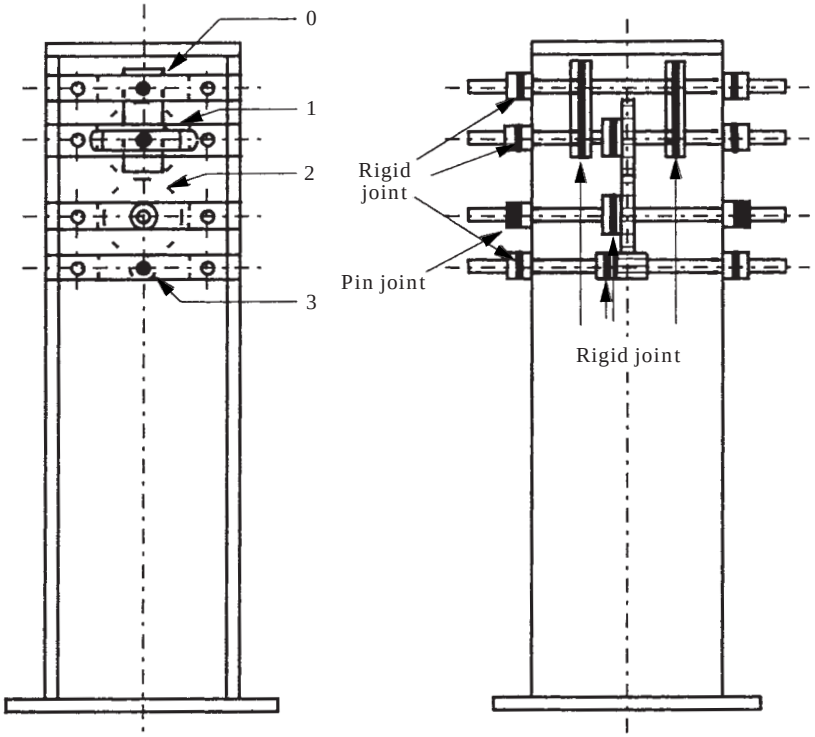

Figure 4. Column used in the experiment: ●, rigid joint; ○, pin joint.

The field transfer matrix for an element of the beam between point $i-1$ to point i is

$$\begin{bmatrix} -w \\ \varphi \\ M \\ V \\ Q \end{bmatrix}_i = \begin{bmatrix} 1 & l & \frac{l^2}{2EJ} & \frac{l^3}{6EJ} - \frac{l}{GA_s} & 0 \\ 0 & 1 & \frac{l}{EJ} & \frac{l^2}{2EJ} & 0 \\ 0 & 0 & 1 & l & 0 \\ 0 & 0 & 0 & 1 & 0 \\ 0 & 0 & 0 & 0 & 1 \end{bmatrix}_i \begin{bmatrix} -w \\ \varphi \\ M \\ V \\ Q \end{bmatrix}_{i-1}, \tag{1}$$

where w is the displacement, φ is the bending slope, M is the bending moment, V is the shearing force, l is the element length, EJ is the flexural rigidity, $GA_s = GA/K_s$ is the shear rigidity, and K_s is the shear coefficient. The point transfer matrix at point i is written by

$$\begin{bmatrix} -w \\ \varphi \\ M \\ V \\ Q \end{bmatrix}_i^R = \begin{bmatrix} 1 & 0 & 0 & 0 & 0 \\ 0 & 1 & 0 & 0 & 0 \\ 0 & 0 & 1 & 0 & 0 \\ m\omega^2 & 0 & 0 & 1 & 0 \\ 0 & 0 & 0 & 0 & 1 \end{bmatrix}_i \begin{bmatrix} -w \\ \varphi \\ M \\ V \\ Q \end{bmatrix}_i^L, \tag{2}$$

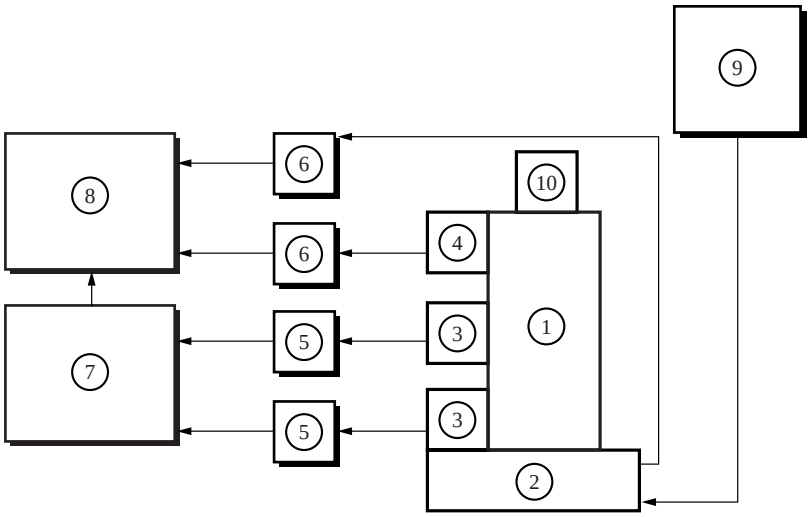

Figure 5. Experimental set-up: ① Column; ② horizontal exciter; ③ strain gage; ④ acceleration pick-up; ⑤ bridge head; ⑥ charge amplifier; ⑦ strain meter; ⑧ oscillograph; ⑨ function generator; ⑩ mass.

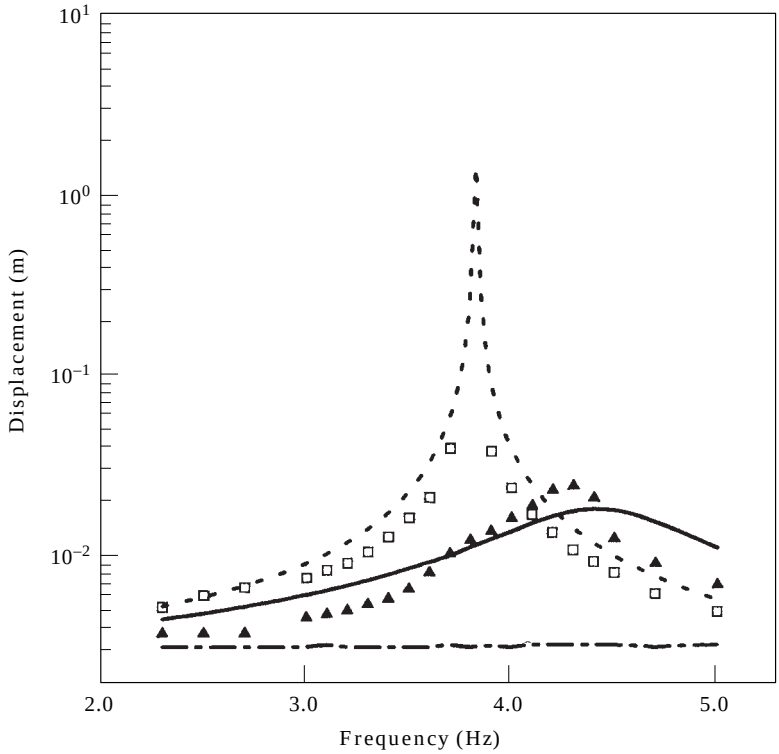

Figure 6. Comparison between theoretical tip displacements and experimental ones: — – —, base displacement; ——, theoretical (with gears); – – –, theoretical (without gears); ▲, experimental (with gears); □, experimental (without gears).

where m_i is the mass at point i and ω is the forced angular frequency. Hence, the matrix at the point 0 is given by

$$\begin{bmatrix} -\bar{w} \\ \bar{\varphi} \\ \bar{M} \\ \bar{V} \\ \bar{Q} \end{bmatrix}^R_i = \begin{bmatrix} 1 & 0 & 0 & 0 & 0 \\ 0 & 1 & 0 & 0 & 0 \\ 0 & 0 & 1 & 0 & l_1 \\ m_0\omega^2 & 0 & 0 & 1 & 1 \\ 0 & 0 & 0 & 0 & 1 \end{bmatrix}_i \begin{bmatrix} -\bar{w} \\ \bar{\varphi} \\ \bar{M} \\ \bar{V} \\ \bar{Q} \end{bmatrix}^L_i, \tag{3}$$

for gear 1 by

$$\begin{bmatrix} -\bar{w} \\ \bar{\varphi} \\ \bar{M} \\ \bar{V} \\ \bar{Q} \end{bmatrix}^R_i = \begin{bmatrix} 1 & 0 & 0 & 0 & 0 \\ 0 & 1 & 0 & 0 & 0 \\ 0 & 0 & 1 & 0 & 0 \\ m_1\omega^2 - jc_1\omega & 0 & 0 & 1 & 0 \\ 0 & 0 & 0 & 0 & 1 \end{bmatrix}_i \begin{bmatrix} -\bar{w} \\ \bar{\varphi} \\ \bar{M} \\ \bar{V} \\ \bar{Q} \end{bmatrix}^L_i, \tag{4}$$

for gear 2 by

$$\begin{bmatrix} -\bar{w} \\ \bar{\varphi} \\ \bar{M} \\ \bar{V} \\ \bar{Q} \end{bmatrix}_R = \begin{bmatrix} 1 & 0 & 0 & 0 & 0 \\ 0 & 1 & 0 & 0 & 0 \\ 0 & 0 & 1 & 0 & 0 \\ m_2\omega^2 - jc_2\omega & 0 & 0 & 1 & -2 \\ 0 & 0 & 0 & 0 & 1 \end{bmatrix}_i \begin{bmatrix} -\bar{w} \\ \bar{\varphi} \\ \bar{M} \\ \bar{V} \\ \bar{Q} \end{bmatrix}_L, \tag{5}$$

and for gear 3 by

$$\begin{bmatrix} -\bar{w} \\ \bar{\varphi} \\ \bar{M} \\ \bar{V} \\ \bar{Q} \end{bmatrix}_R = \begin{bmatrix} 1 & 0 & 0 & 0 & 0 \\ 0 & 1 & 0 & 0 & 0 \\ 0 & 0 & 1 & 0 & -r_3 \\ m_3\omega^2 - jc_3\omega & 0 & 0 & 1 & 1 \\ 0 & 0 & 0 & 0 & 1 \end{bmatrix}_i \begin{bmatrix} -\bar{w} \\ \bar{\varphi} \\ \bar{M} \\ \bar{V} \\ \bar{Q} \end{bmatrix}_L. \tag{6}$$

There is a lot of friction at the contact point between gear teeth because the gear teeth make sliding motions, and it gives damping in the system. In the above

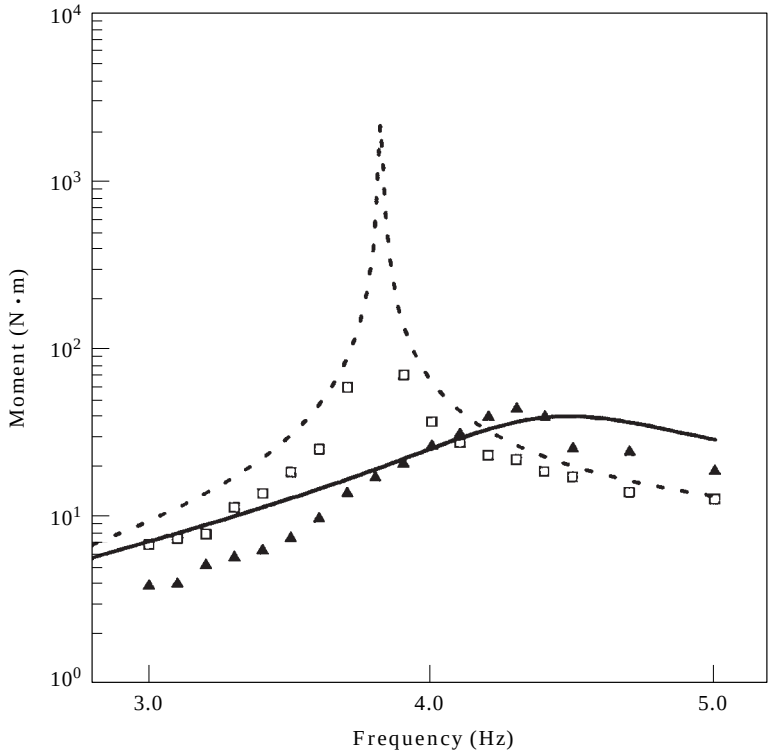

Figure 7. Comparison between theoretical bending moments at the base of the column and experimental ones: ——, theoretical (with gears); – – –, theoretical (without gears); ▲, experimental (with gears); □, experimental (without gears).

TABLE 1

Dimensions used in the numerical simulation for the experimental model

Masses of the intelligent column (kg)	Segment mass of:	
	Column	$m_1 = 0{\cdot}630$
	Rigid arm	$m_0 = 0{\cdot}557$
	Gear 1	$m_1 = 0{\cdot}891$
	Gear 2	$m_2 = 1{\cdot}337$
	Gear 3	$m_3 = 0{\cdot}835$
Radius of the gears (mm)	Gear 1	$r_1 = 31{\cdot}0$
	Gear 2	$r_2 = 31{\cdot}0$
	Gear 3	$r_3 = 8{\cdot}50$
Equivalent damping coefficients between the gears (N · s/m)	Gear 1	$c_1 = 15{\cdot}0$
	Gear 2	$c_2 = 15{\cdot}0$
	Gear 3	$c_3 = 54{\cdot}7$
Torsional rigidity of the shaft for gear 3 (N · m/rad)	$K_0 = 2{\cdot}8$	
Base displacement (mm)	3·18	
Size (mm × mm × mm)	500 × 150 × 150	

TABLE 2

Dimensions of the beam with hollow-square cross-section used in the optimal design

Length in the axial direction (mm)	4000
Length of the cross-section (mm)	310
Width of the cross-section (mm)	310
Thickness of the beam (mm)	5
Thickness of the gear (mm)	300
Radii of the shaft (mm)	100 (shaft for gear 1)
	100 (shaft for gear 2)
	90 (shaft for gear 3)
Module of gears (mm)	12
Mass on the top of the beam (kg)	1000
Mass of the beam (kg)	190

equations c_1–c_3 are the equivalent damping coefficients for the friction of gear 1 through gear 3, and $j = \sqrt{-1}$. The upper line of each state variable denotes the complex number, and m_0, m_1, m_2 and m_3 are the masses at points 0, 1, 2 and 3, respectively (see Figure 1), l_1 is the length of the rigid arm, r_3 is the radius of the pitch circle of gear 3, and c_1, c_2 and c_3 are the damping coefficients at points 1, 2 and 3, respectively.

Let the beam be a cantilever beam whose base is built-in and the other end is free, but carrying a concentrated mass. The boundary conditions are

$$-w_0' = u_0, \qquad -w_0^i = 0, \qquad \varphi_0^r = 0, \qquad \varphi_0^i = 0, \tag{7a}$$

$$M^r = 0, \qquad M^i = 0, \qquad V^r = 0, \qquad V^i = 0. \tag{7b}$$

The transfer matrix involves the tip mass, so the boundary condition equation (7b) denotes the values at an upper point of the mass. The subscript r denotes the values of the real part, and i the imaginary, and u_0 the amplitude of sinusoidal forced displacement. The matrix $\bar{\mathbf{B}}$ which connects point o to point T is written by

$$\begin{bmatrix} -\bar{w} \\ \bar{\varphi} \\ 0 \\ 0 \\ \bar{Q} \end{bmatrix}_T = \begin{bmatrix} B_{11} & \cdots & \cdots & \cdots & B_{15} \\ \vdots & \ddots & & & \vdots \\ \vdots & & \ddots & & \vdots \\ \vdots & & & \ddots & \vdots \\ B_{51} & \cdots & \cdots & \cdots & B_{55} \end{bmatrix} \begin{bmatrix} \bar{u} \\ 0 \\ \bar{M} \\ \bar{V} \\ \bar{Q} \end{bmatrix}_0, \tag{8}$$

TABLE 3

Optimal parameters for the gear mechanism obtained by the optimal design method

	Before optimization	After optimization
Diameter of pitch circle of gear 1 (mm)	204	228
Diameter of pitch circle of gear 2 (mm)	204	212
Diameter of pitch circle of gear 3 (mm)	204	180
Location of the rigid arm (mm)	2000	3046

from which

$$\left.\begin{aligned} B_{31}\bar{u}_0 + B_{33}\bar{M}_0 + B_{34}\bar{V}_0 + B_{35}\bar{Q}_0 = 0 \\ B_{41}\bar{u}_0 + B_{43}\bar{M}_0 + B_{44}\bar{V}_0 + B_{45}\bar{Q}_0 = 0 \end{aligned}\right\}. \tag{9}$$

Then one has

$$\begin{aligned} \bar{M}_0 &= \frac{1}{B_{33}B_{44} - B_{34}B_{43}} \\ &\quad \times \{(B_{34}B_{41} - B_{31}B_{44})\bar{u}_0 + (B_{34}B_{45} - B_{35}B_{44})\bar{Q}_0\} \\ \bar{V}_0 &= \frac{1}{B_{33}B_{44} - B_{34}B_{43}} \\ &\quad \times \{(B_{31}B_{43} - B_{33}B_{41})\bar{u}_0 + (B_{35}B_{43} - B_{33}B_{45})\bar{Q}_0\} \\ -\bar{w}_0 &= \bar{u}_0 \\ \bar{\varphi}_0 &= 0. \end{aligned} \tag{10}$$

3.2. METHOD OF CALCULATING REACTION FORCE Q

In the above equations, the reaction force Q should be decided for calculating the response of the beam. The horizontal displacement of the contact point between gear 1 and gear 2 is (see Figure 3)

$$w_1 - r_1\varphi_1, \tag{11}$$

where w_1 is the displacement of gear 1 in the horizontal direction. The horizontal displacement at the contact point is also written by using the values of gear 2:

$$w_2 + r_2\varphi_2 + r_2\theta_2. \tag{12}$$

Equation (11) is equal to equation (12), so one has

$$w_1 - r_1\varphi_1 = w_2 + r_2\varphi_2 + r_2\theta_2. \tag{13}$$

Gear 3 is driven by gear 2, so there is the following relation:

$$r_2\theta_2 = r_3\theta_3 + r_3\varphi_3. \tag{14}$$

The moment due to the force Q is equal to the restoring torque at gear 3:

$$r_3\bar{Q} - \bar{K}_\theta\bar{\theta}_3 = 0, \tag{15}$$

where r_1, r_2 and r_3 are the radii, θ_1, θ_2 and θ_3 are angles of rotation of gears 1, 2 and 3, respectively, and K_θ is the rotational spring constant at gear 3 due to the shaft which makes the connection of gear 3 to the column. Equation (15) is rewritten by

$$\left.\begin{aligned} X(1) &= \mathrm{Re}\,(r_3\bar{Q} - \bar{K}_\theta\bar{\theta}_3) = 0 \\ X(2) &= \mathrm{Im}\,(r_3\bar{Q} - \bar{K}_\theta\bar{\theta}_3) = 0 \end{aligned}\right\}, \tag{16}$$

TABLE 4

Parameters used in the calculation of frequency response for the optimal beam

Masses of the intelligent column (kg)	Mass above the gear mechanism	$m_1 = 4{\cdot}54$
	Mass under the gear mechanism	$m_1 = 11{\cdot}50$
	Rigid arm	$m_0 = 98{\cdot}10$
	Gear 1	$m_1 = 105{\cdot}0$
	Gear 2	$m_2 = 99{\cdot}10$
	Gear 3	$m_3 = 82{\cdot}60$
Radius of the gears (mm)	Gear 1	$r_1 = 114{\cdot}0$
	Gear 2	$r_2 = 108{\cdot}0$
	Gear 3	$r_3 = 90{\cdot}0$
Equivalent damping coefficients between the gears (N · s/m)	Gear 1	$c_1 = 6{\cdot}00 \times 10^3$
	Gear 2	$c_2 = 6{\cdot}00 \times 10^3$
	Gear 3	$c_3 = 7{\cdot}60 \times 10^3$
Torsional rigidity of the shaft for gear 3 (N · m/rad)		$K_0 = 1{\cdot}68 \times 10^6$
Base displacement (mm)		15·0

where Re denotes the real part, and Im the imaginary part. The angle θ_3 is obtained by equations (13) and (14):

$$\theta_3 = \frac{r_2}{r_3}\left\{\frac{w_1 - r_1\varphi_1}{r_2} - \varphi_2 - \frac{w_2}{r_2}\right\} - \varphi_3.$$

Equation (16) cannot be solved analytically, because the displacements and bending slopes are included in a matrix with complex numbers. Equation (16) is solved numerically by using the Brent method which is applicable to non-linear equations.

4. COMPARISON BETWEEN EXPERIMENTAL AND NUMERICAL RESULTS

4.1. EXPERIMENTAL SET-UP

To validate the method, experimental tests have been carried out for a vertical beam (a column). The column used in the experiment is made up of two steel plates of thickness 3 mm, as shown in Figure 4. In the figure, the arm (the rigid lever) made of steel with high rigidity is rigidly connected to the top of the column, and the shaft of gear 3 is rigidly connected to the column and gear 3. There is a slit for the support plates which support the shaft of gear 1, so gear 1 moves in the

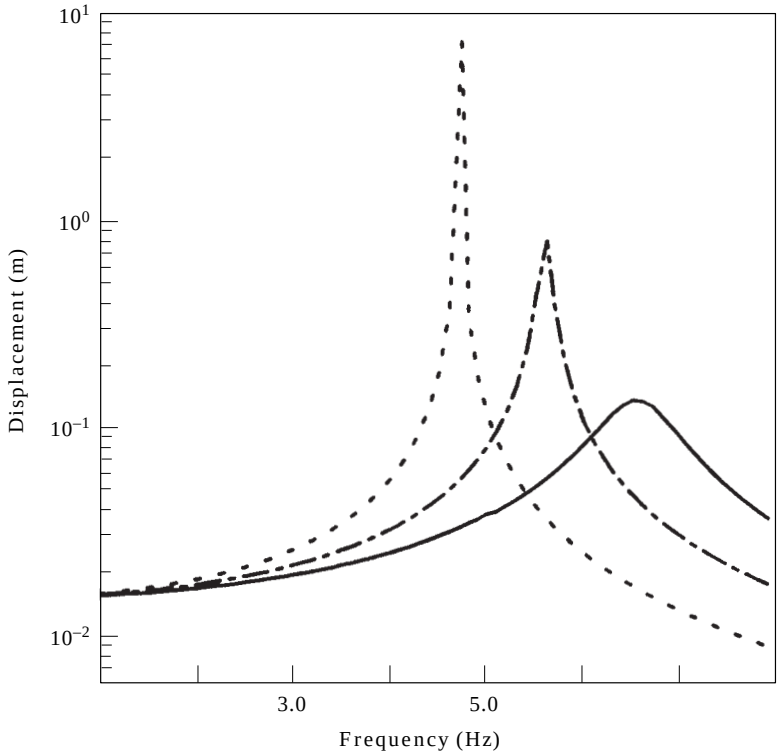

Figure 8. Frequency response of the tip displacements of the beam treated in the optimal design: ——, with gears (after optimization); – – –, with gears (before optimization); —, without gears.

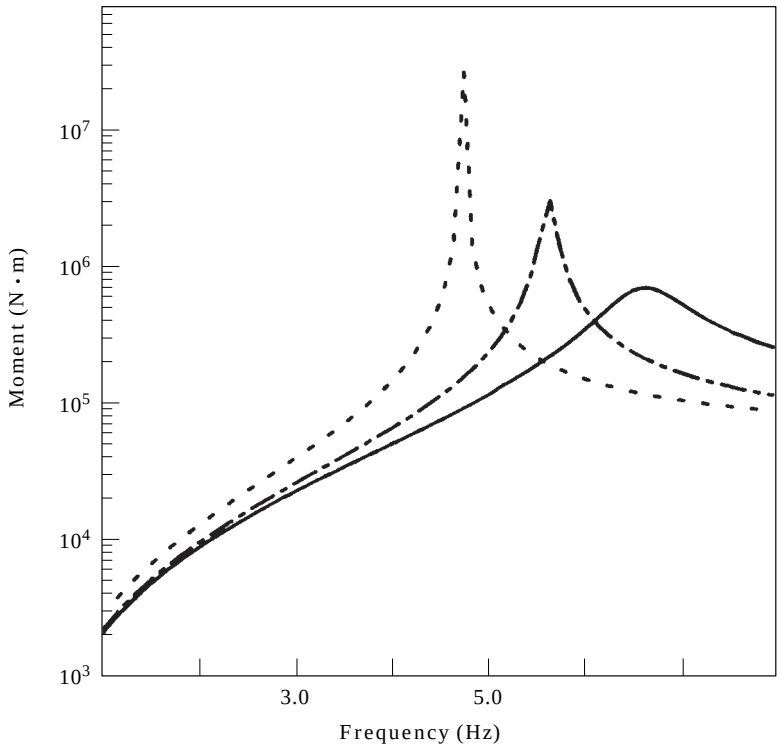

Figure 9. Frequency response of the bending moments at the base of the beam treated in the optimal design: ——, with gears (after optimization); — – —, with gears (before optimization); – – –, without gears.

horizontal direction with the arm. Gear 2 can rotate around its axis freely, so the movement of gear 1 is transmitted to gear 3 passing through gear 2, but the rotating direction is changed by the middle gear 2. The height of the column is 500 mm, the length is 150 mm, the width is 150 mm, and the mass of the column is 7·4 kg. A mass of 3·75 kg is laid on the top of the column, and the base of the column is fixed on the table of horizontal oscillator. The column without gears having the same sizes is also made. The mass of the column is 5·6 kg.

Figure 5 depicts the experimental set-up, in which the tip displacement and the strain at the base are measured. To detect the displacement, an acceleration sensor is used. The displacement is obtained by integrating the acceleration signal twice. The strain is measured by using the dynamic strain-meter. These values are input to a memory oscilloscope, and time response curves are generated by using a printer. The measured data are depicted by white squares and black triangles in Figures 6 and 7.

4.2. NUMERICAL CALCULATION

To validate the present analysis, numerical calculations are carried out for the same model used in the experiment. Since there is a great deal of friction between the gear teeth, and it varies with the forces applied to the gear teeth, the damping coefficient c_1 is decided by reference to the experimental data. The other

coefficients are decided by using the gear ratios. Take, for instance, the damping coefficient between the middle gear 2 and the fixed gear 3, given by

$$c_3 = (r_1/r_3) \cdot c_1. \tag{17}$$

Table 1 depicts the dimensions used in the numerical calculation which are related to the experimental column. Numerical results are depicted by the solid and dotted lines in Figures 6 and 7.

4.3. COMPARISON BETWEEN THE NUMERICAL AND THE EXPERIMENTAL RESULTS

Figure 6 shows the frequency response curve at the tip of the column when the base is excited. In the figure, □ shows the experimental data for the column without gear mechanism, and ▲ shows the curve for the present column with the gear mechanism, and the chain line shows the amplitude of the base displacement. The resonance frequency for the present column is larger than that of the column without gears, and the amplitude at resonance is significantly suppressed for the present column due to the friction among gear teeth. Especially for frequencies less than the resonance frequency, the displacement amplitude is significantly smaller for the present column in comparison with the column without gears.

Figure 7 shows the frequency response of the bending moments at the base of the column. The marks represent the experimental data, and lines represent the theoretical results. The resonance peak is also suppressed in this figure, and the experimental data for the present column in the low frequency region are significantly smaller than those of the column without gears. In designing the column used in the usual structures, resonance is avoided, and the principal frequencies of the disturbances, such as earthquakes, are less than the natural frequency of the structure, so the bending moments in low frequencies less than the resonance frequency should be suppressed. In the present column, the bending moments in the low frequency region can be suppressed, so the present column has advantages.

Although a few discrepancies are found between the experimental and the theoretical results, both sets of results are in good agreement from the design engineering point of view, and the analytical results can be used in the design of the present column.

5. METHOD OF OPTIMAL DESIGN

It has been ascertained that the present beam or column has advantages for controlling vibrations of structures excited by earthquakes. However, the system is not optimum. For the column, effects of vibration control will increase when parameters such as the gear ratio and the location of the gear mechanisms are chosen to be optimal values. In this case a method of optimal design is discussed below.

5.1. MODEL OF THE COLUMN

The above model used in the experiment is different from actual structures, because the weight and the height of the beam are limited due to the capacity of the oscillator. In the present section, sizes near the actual beams are chosen: length = 4 m, size of the cross-section = 31 × 31 cm, and thickness = 5 mm. The mass of the gear mechanism is 500 kg, and the concentrated mass 1000 kg lies at the tip of the beam which is made of steel. Details of the beam are given in Table 2. The allowable stresses are chosen as follows: $\sigma_b = 392\ \mathrm{N/mm^2}$ for the normal stress of gear teeth, and $\tau_a = 98\ \mathrm{N/mm^2}$ for the shear stress for the shaft. The module of the gears is taken as 12.

In the optimal design the stresses are limited within the above values. The usual design method of gears is used. The calculated minimum diameters of the pitch circle are D_1, $D_2(\min) = 183$ mm, and $D_3(\min) = 173$ mm, the minimum number of gear teeth are Z_1, $Z_2 = 15{\cdot}25$, $Z_3 \fallingdotseq 14{\cdot}42$. Then one takes Z_1, $Z_2 = 16$, $Z_3 = 15$, and the minimum pitch diameters are D_1, $D_2 = 192$, $D_3 = 180$ mm. The inner space of the hollow square beam is 300 × 300 mm, so the regions for the pitch diameters yield:

$$\left.\begin{array}{c} 192 \leqslant D_1, D_2 \leqslant 228 \\ 180 \leqslant D_3 \leqslant 228 \end{array}\right\}.$$

The control effect is small when the shaft of the rigid arm lies in the low position, so the minimum length from the base at the shaft is taken to be 1·5 m, the maximum length is also limited by the geometrical relations, and it becomes 3·8 m. Hence, the region for searching the optimal value for the location is 1·5 m ⩽ length from the base for the shaft of the rigid arm ⩽ 3·8 m.

5.2. COST FUNCTION

Since the beam is destroyed near the base due to the bending moment in earthquakes, the cost function is chosen for decreasing the bending moments at the base of the beam. The forces acting on the gear teeth become large as the control force increases, and it is often difficult to design the gear mechanism because sizes of gears are limited in the hollow pipe. Vibrations can be suppressed when the frequency response curve is suppressed in the frequency domain. From this situation, the following cost function is chosen:

$$J = \alpha_1 \int_{\omega_1}^{\omega_2} |M(\omega)|\, \mathrm{d}\omega + \alpha_2 \int_{\omega_1}^{\omega_2} |Q(\omega)|\, \mathrm{d}\omega, \tag{18}$$

where $M(\omega)$ is the bending moment at the base of the beam, $Q(\omega)$ is the reaction force which acts on the gear teeth, α_1 and α_2 are the weights, ω is the forced angular frequency, and ω_1 and ω_2 are the lower and upper bounds in the considered frequency region. Equation (18) means that the bending moment at the base becomes minimum under the minimum reaction force when the cost function J is minimized. Equation (18) is the non-linear equation, so the numerical iteration

method is applied. Table 3 depicts the calculated optimal parameter (values of pitch diameters of gears and the location of the shaft of the rigid arm measured from the base). In Table 3, the initial values of the parameters before the optimization are also depicted. Optimal values are remarkably different from the initial values, so the optimal design will be of importance in the design of the present beam.

In Table 3, the tooth number of gear 2 with pitch diameter 212 mm is 17·67, so that $D_2 = 216$ mm ($Z = 18$) is applied in the calculation. The rotational spring constant of the shaft is $K_\theta = (G\pi d^4/32l)$, where G is the shear modulus, d is the diameter, and l is the length of the shaft. It is difficult to estimate the damping coefficients because those values are decided by reference to the experimental data. In the present calculation, the values are assumed by reference to the previous experimental data. Figure 4 shows the data used in the numerical simulation in the optimal design problem.

5.3. NUMERICAL RESULTS UNDER THE OPTIMAL DESIGN

Figure 8 shows the frequency response of the tip displacement of the beam. Three cases are depicted in the figure, one is the result for the beam without gears (dashed line), the second is for the beam with the gear mechanism but without optimization (chain line), and the third is for the beam with the optimal gear mechanism (solid line). The resonance peak for the optimal gear mechanism moves to the high frequency zone. Since the principal frequencies of earthquakes in Japan are in the region of 2·5 to 4·5 Hz, the optimization is made in the region. Then the amplitudes of the tip displacements for the optimal gear mechanism are quite small in the region in comparison with two others.

Figure 9 depicts the frequency response of the bending moments at the base of the beam. The results in three cases are shown. The tendency is similar to the displacement. However, the bending moments for the beam with the optimal gear mechanism in the target frequencies (2·5 through 4·5 Hz) are remarkably smaller than those of the beam without gears. Since the beam is collapsed by the bending moments at the base, small bending moments at the base are desirable. The moments are suppressed within about 47% of those for the beam without gears in the target frequencies, so the method using the cost function involving the bending moments is valid in the design of the present beam.

The results obtained are based on the analysis of steady state vibrations. The earthquake wave involves higher modes and has noisy shape, so the wave is different from the sinusoidal one. In this study, the principle of the proposed system is proven, and the results obtained are different from those under the earthquake waves.

In the real column, since the earthquake force is large, there are effects of deformations of gears. But the effects can be neglected from the design engineering point of view, because the deformations of gear teeth are small in comparison with those of the column when the gears are designed with consideration of the appropriate safety factor.

6. CONCLUSION

An intelligent beam is presented, in which the earthquake force is transformed into vibration control force by using the gear mechanism, without using sensors. Theoretical analysis was carried out on the beam, and the results for obtaining the required response have been presented. To validate the present system and the analytical results, experimental tests were carried out for a model of the beam. It was ascertained that the present system suppresses vibrations of the beam. The optimal design method for the beam has been presented. In the method, the cost function was used in which both the bending moments at the base and the reaction force at the gear teeth are included. The optimal parameters, such as the pitch diameters of the gears and the position of the gears, have been calculated for a beam whose size corresponds to actual structures. It has been ascertained that the optimal beams can be designed by using the present method.

REFERENCES

1. S. Xue, J. Tobita, S. Kurita and M. Izumi 1997 *Journal of Engineering Mechanics* **123**, 322–327. Mechanics and dynamics of intelligent passive vibration system.
2. J. Prendergast 1995 *Civil Engineering* **65**, 58–61. Seismic isolation in bridges.
3. G. Lee-Glauser, G. Ahmadi and Lucas G. Horta 1997 *Journal of Structural Engineering* **123**, 499–504. Integrated passive/active vibration absorber for multistory buildings.
4. R. Villaverde Koyama and A. Leslie 1993 *Earthquake Engineering and Structural Dynamics* **22**, 491–507. Damped resonant appendages to increase inherent damping in buildings.
5. F. Sadek, B. Mohraz and A. W. Taylor 1997 *Earthquake Engineering and Structural Dynamics* **26**, 617–635. A method of estimating the parameters of tuned dampers for seismic applications.
6. S. Utku, B. Utku and B. K. Wada 1993 *Earthquake Engineering and Structural Dynamics* **22**, 823–827. A readily available energy source for active vibration control in buildings.
7. A. Ohsumi and Y. Sawada 1993 *Journal of Dynamic Systems, Measurement and Control* **115**, 649–657. Active control of flexible structures subject to distributed and seismic disturbances.
8. C.-H. Chung, D.-N. Wu and Q. Wang 1996 *Journal of Dynamic Systems, Measurement and Control* **118**, 113–119. LQR for state-bounded structural control.
9. M. Q. Feng and A. Mita 1995 *Journal of Engineering Mechanics* **121**, 1082–1088. Vibration control of tall buildings using mega-subconfiguration.